THE JOURNAL OF BIOLOGICAL CHEMISTRY VOL. 287, NO. 47, pp. 39505–39512, November 16, 2012

Tic22 Is an Essential Chaperone Required for Protein Import into the Apicoplast*[S]

Received for publication, July 26, 2012, and in revised form, September 28, 2012 Published, JBC Papers in Press, October 1, 2012, DOI 10.1074/jbc.M112.405100

Stephanie Glaser[‡1,2], **Giel G. van Dooren**[§1,3], **Swati Agrawal**[¶4], **Carrie F. Brooks**[‖], **Geoffrey I. McFadden**[**5], **Boris Striepen**[¶‖6], **and Matthew K. Higgins**[‡‡7]

From the [‡]*Department of Biochemistry, University of Cambridge, Cambridge, CB2 1GA, England, the* [§]*Research School of Biology, Australian National University, Canberra, ACT, 0200, Australia, the* [¶]*Department of Cellular Biology and* [‖]*Center for Tropical and Emerging Global Diseases, University of Georgia, Athens, Georgia 30602, the **Plant Cell Biology Research Centre, School of Botany, University of Melbourne, Parkville, Victoria, 3010, Australia, and the* [‡‡]*Department of Biochemistry, University of Oxford, South Parks Road, Oxford, OX1 3QU, England*

Background: Tic22 is a core protein import machinery component of chloroplasts and apicoplasts.
Results: Tic22 is a chaperone, required for parasite survival and for protein import in the apicoplast.
Conclusion: Tic22 lies between the plastid membranes, maintaining imported proteins unfolded for translocation.
Significance: Chaperones which hold proteins in an unfolded state are central to membrane translocation systems and Tic22 plays this role in plastids.

Most plastids proteins are post-translationally imported into organelles through multisubunit translocons. The TIC and TOC complexes perform this role in the two membranes of the plant chloroplast and in the inner two membranes of the apicoplasts of the apicomplexan parasites, *Toxoplasma gondii* and *Plasmodium falciparum*. Tic22 is a ubiquitous intermembrane translocon component that interacts with translocating proteins. Here, we demonstrate that *T. gondii* Tic22 is an apicoplast-localized protein, essential for parasite survival and protein import into the apicoplast stroma. The structure of Tic22 from *P. falciparum* reveals a fold conserved from cyanobacteria to plants, which displays a non-polar groove on each side of the molecule. We show that these grooves allow Tic22 to act as a chaperone. General chaperones are common components of protein translocation systems where they maintain cargo proteins in an unfolded conformation during transit. Such a chaperone had not been identified in the intermembrane space of plastids and we propose that Tic22 fulfills this role.

Endosymbiosis has been a major driver of eukaryotic evolution. Plastids, such as the chloroplasts of plants, evolved through the endosymbiotic acquisition of a cyanobacterium by a eukaryotic cell. Plastids are critical to the survival of cells in which they are found, and have central roles in carbon fixation and synthesis of biomolecules such as tetrapyrroles, amino acids, fatty acids, and isoprenoids. After the initial endosymbiosis that led to the evolution of primary plastids in plants and red algae, plastids spread through multiple eukaryotic phyla through a number of secondary endosymbioses. Here, a plastid-bearing eukaryote became incorporated into a heterotrophic eukaryote, bestowing the many biochemical advantages of a plastid. Plastids derived in this manner are found in organisms as diverse as brown algae, dinoflagellates, and a group of intracellular parasites called the Apicomplexa. Apicomplexa include *Plasmodium* spp., the causative agents of malaria, and *Toxoplasma gondii*, the cause of toxoplasmosis. They contain a plastid known as the apicoplast (1). Although highly reduced in function compared with the chloroplasts of plants, apicoplasts are critical for parasite survival as they contain essential enzymatic pathways for the synthesis of fatty acids, heme, iron-sulfur clusters, and isoprenoids (2).

Most proteins that function in plastids are encoded by nuclear genes and are post-translationally trafficked by multisubunit translocons across the two or more membranes that surround the organelle (3). In plant chloroplasts, this is mediated by the Translocons of the Inner and Outer Chloroplast membranes (the TIC[8] and TOC complexes). The TOC complex recognizes motifs in plastid-targeted proteins and feeds them through the pore formed by the β-barrel of Toc75 (3). Reconstitution of just Toc75 and Toc159 into liposomes generates a functional import apparatus, suggesting that the TOC complex can act independently of any other components to drive proteins across the outer membrane (4). *In vivo*, some proteins are completely translocated through the TOC complex before engaging the inner membrane TIC complex (5),

* This work was funded by an Australian Research Council Discovery grant (to G. v. D.), a National Health and Medical Research Council Program Grant (to G. I. M.), a Medical Research Council grant (to M. K. H.), and a grant from the National Institutes of Health (AI 64671) (to B. S.).
The atomic coordinates and structure factors (code 4E6Z) have been deposited in the Protein Data Bank (http://wwpdb.org/).
[S] This article contains supplemental Figs. S1–S7.
[1] Both authors contributed equally to this work.
[2] Supported by a Medical Research Council Studentship.
[3] A QEII Fellow of the Australian Research Council. To whom correspondence may be addressed. E-mail: giel.vandooren@anu.edu.au.
[4] Supported by a predoctoral fellowship from the American Heart Association. Present address: Dept. of Microbiology and Immunology, University of Michigan, Ann Arbor, MI 48105.
[5] An ARC Federation Fellow.
[6] A Georgia Research Alliance Distinguished Investigator. To whom correspondence may be addressed. E-mail: striepen@uga.edu.
[7] To whom correspondence may be addressed. E-mail: matthew.higgins@bioch.ox.ac.uk.

[8] The abbreviations used are: TIC, translocons of the inner chloroplast membranes; TOC, translocons of the outer chloroplast membranes; ATc, anhydrotetracycline.

while proteins destined for the intermembrane space use the TOC complex alone to reach their final destination (6). More commonly, proteins are translocated simultaneously across both TIC and TOC complexes at contact sites (7), engaging with the TIC machinery before completing their passage through Toc75 (4).

The TIC complex of plants is thought to consist of at least seven subunits, although their functions and association with one another are not well understood. Both Tic110 and Tic20 have been proposed to serve as pores, although they may be part of different TIC complexes (8, 9). The TIC complex of plants also contains subunits that likely function in redox regulation, a subunit (Tic40) that recruits the chaperone ClpC to the stromal (inside) side of the TIC complex to mediate protein translocation, and a subunit of unknown function called Tic22 (10–12).

Tic22 was originally identified through association with plastid-targeted proteins in cross-linking studies (12, 13). It is a 22 kDa protein that localizes to the chloroplast intermembrane space. Although Tic22 is soluble, it is found in inner membrane preparations and a small percentage co-fractionates with the integral inner membrane component Tic20 (12). Tic22 also interacts with Toc64, and cofractionates with the TOC complex (12, 14). Whether these interactions occur simultaneously or transiently is uncertain, and roles for Tic22 in either bridging the TIC and TOC complexes, or in shuttling translocated proteins between the two have been proposed (3). A recent study of a cyanobacterial Tic22 homologue proposes a role of Tic22 in bacterial outer membrane biogenesis, perhaps functioning as a chaperone (15).

Apicoplasts are bound by four membranes, the inner two of which are homologous to the two membranes that surround plant chloroplasts. As in primary plastids, each apicoplast membrane appears to contain a translocon that mediates protein import. Apicomplexan genomes contain homologues of subunits of both the TIC and TOC complexes (1, 16–18). The apicomplexan homologue of Tic20 localizes to the inner apicoplast membrane and is essential for parasite survival and for protein import (18). Apicomplexan genomes also harbor a plastid-targeted Tic22 homologue and an, as yet, uncharacterized homologue of Toc75 (16, 17). The presence of these homologues suggest that protein translocation across the inner two membranes of apicoplasts is similar to that in plants. Furthermore, conservation of these TIC and TOC homologues across vast evolutionary distances suggests that they most likely represent "core" components of the plastid import machinery.

Although Tic22 is ubiquitous in plastids of plants, algae and Apicomplexa parasites, its function and importance during protein import are unknown. In this study, we combine genetics and structural biology to define the function of Tic22. We use targeted genome manipulation in *Toxoplasma* to demonstrate a requirement for Tic22 in apicoplast protein import. We then establish the structure of Tic22 in the related parasite *P. falciparum* and show that Tic22 from both *Toxoplasma* and *Plasmodium* act as chaperone proteins.

EXPERIMENTAL PROCEDURES

T. gondii parasites were cultured in human foreskin fibroblasts with Dulbecco's modified Eagles medium, supplemented with 1% fetal bovine serum and antibiotics. Where relevant, we added anhydrotetracycline to the growth medium at a final concentration of 0.5 μg/ml. Parasite manipulations and mutant generation was performed as previously described (18). Details of *Tg*Tic22 cloning and vector construction and parasite genetic modifications are described in the supplemental information.

Growth assays were performed using a SpectraMax M2^e microplate reader (Molecular Devices) as previously described (18). For measuring apicoplast biogenesis in the *Tg*Tic22 mutant, we introduced an apicoplast-targeted red fluorescent protein (18). We counted 100 four-cell vacuoles at each time point and measured parasites for the presence or absence of an apicoplast. Pulse-chase data were analyzed by autoradiography and PhosphorImaging (GE Healthcare). To quantify the level of import in the pulse-chase assays for *Tg*Cpn60 and FNR-mD-HFR-cmyc, we calculated the ratio of the amount of mature protein in the chase lane to the amount of precursor in the pulse lane. To quantify the amount of *Tg*PDH-E2-LA, we compared the amount of *Tg*PDH-E2-LA to the amount of lower mito-E2-LA band in the chase lanes. To enable comparison between different import assays, we normalized the data, setting the no ATc value to 100%. Band intensities were quantified using either ImageJ or PhosphorImaging software.

Western blotting, pulse-chase analyses, immunoprecipitations, immunofluorescence assays, sodium carbonate extractions, and TX-114 partitioning were all performed as previously described (18, 19). We used the following antibodies for Western blotting, immunoprecipitations, and immunofluorescence assays: rabbit anti-*Tg*ACP, rat anti-HA (Roche), mouse anti-c-Myc (Roche and Santa Cruz Biotechnology), mouse anti-TgGRA8 (a kind gift from Gary Ward, University of Vermont), rabbit anti-*Tg*Cpn60, rabbit anti-MIC5 (a kind gift from Vern Carruthers, University of Michigan), and rabbit anti-lipoic acid (Calbiochem). Secondary antibodies used for immunofluorescence assays were goat anti-rabbit Alexa Fluor 546 (1:500), goat anti-mouse Alexa Fluor 546 (1:500), goat anti-mouse Alexa Fluor 647 (1:200), and goat anti-rat Alexa Fluor 488 (1:200; Invitrogen). Parasites were imaged using a DeltaVision set-up on an inverted Olympus IX71 microscope fitted with an Olympus objective lens (UPlanSApo 100x/1.40 Oil), with images recorded using a Photometrics CoolSNAP HQ or HQ^2 camera. Images were deconvolved and adjusted for contrast.

*Pf*Tic22 was expressed, purified, and crystallized as described (20) with a selenomethionine derivative used to derive phase information. *Tg*Tic22 was also expressed in *Escherichia coli* and purified. Insulin aggregation assays were performed by mixing insulin and Tic22 proteins at defined ratios, inducing insulin aggregation by the addition of DTT and following light scattering at 360 nm. Detailed procedures are included in SI "Experimental Procedures."

RESULTS

A Toxoplasma gondii Homologue of Tic22—Using BLAST searches with plant and algal sequences as queries, we identified a single Tic22 homologue in the *T. gondii* genome. Initial alignments suggested that the computational gene model (TGME49_08605, www.toxodb.org) may be incomplete and we

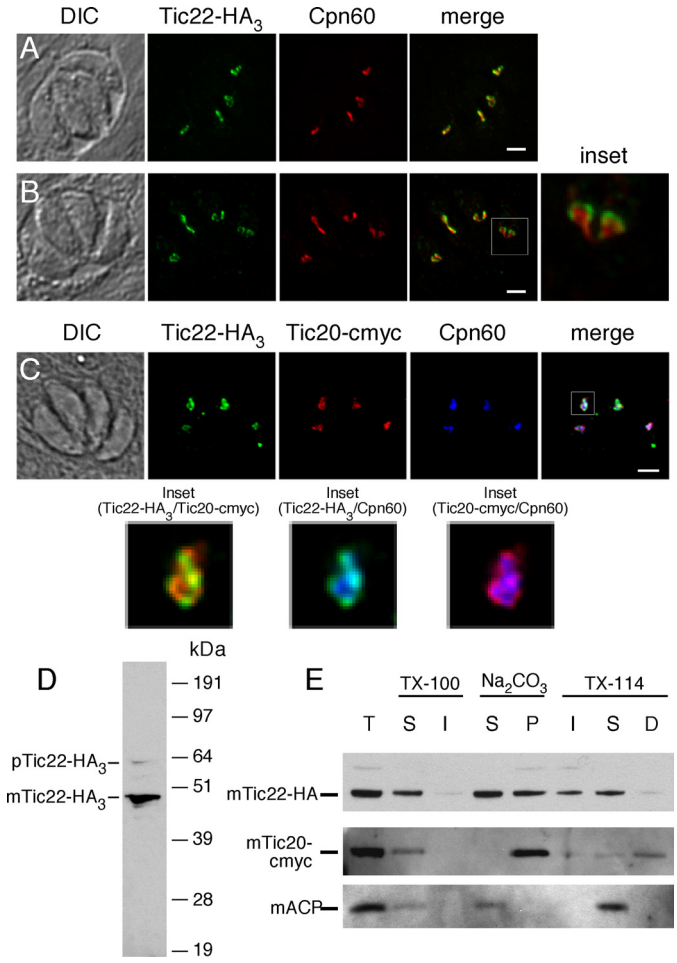

FIGURE 1. **TgTic22 is a soluble protein of the apicoplast periphery.** *A* and *B*, immunofluorescence assay depicting *Tg*Tic22-HA (*green*) and the stromal apicoplast marker *Tg*Cpn60 (*red*). The *inset* in *B* highlights the peripheral labeling of *Tg*Tic22-HA relative to *Tg*Cpn60. *C*, immunofluorescence assay depicting *Tg*Tic22-HA (*green*), *Tg*Cpn60 (*blue*), and the apicoplast inner membrane protein *Tg*Tic20-cmyc (*red*). The insets below highlight the peripheral labeling of both *Tg*Tic22-HA and *Tg*Tic20-cmyc relative to *Tg*Cpn60. Scale bar on all images is 2 μm. *D*, Western blot of *Tg*Tic22-HA protein reveals a major protein band at around 49 kDa, and a minor, pre-processed band at around 60 kDa. *E*, determination of the solubility of *Tg*Tic22-HA relative to the integral membrane protein *Tg*Tic20-cmyc and the soluble apicoplast protein *Tg*ACP. Parasite protein extracts were separated into TX-100 soluble (*S*) and insoluble (*I*) fractions, sodium carbonate (Na_2CO_3) soluble (*S*) and integral membrane pellet (*P*) fractions, and TX-114 insoluble (*I*), soluble (*S*) and detergent (*D*) fractions.

performed 5′- and 3′-rapid amplification of cDNA ends (RACE) to establish the entire open reading frame (GenBank™ accession number JX025072). The putative *Tg*Tic22 consists of five exons, encoding a 62 kDa protein. This is considerably larger than other known Tic22 homologues due to the presence of a large N-terminal extension and several insertions of low complexity sequence (supplemental Fig. S1).

TgTic22 Is a Soluble Protein of the Apicoplast Periphery—To localize TgTic22, we introduced a 3× hemagglutinin (HA) tag into the 3′-end of the Tic22 genomic locus using a cosmid recombineering system (21). We generated genetically modified parasites expressing this construct and used immunofluorescence to localize *Tg*Tic22. This revealed that *Tg*Tic22 is located near the apicoplast stromal marker Cpn60 (Fig. 1, *A–C*; (19)). The apicoplast is a dynamic organelle that changes shape considerably during the cell cycle (22). When the apicoplast is large in size, such as during organellar division, it is possible to distinguish between peripheral and stromal proteins. In such large apicoplasts, *Tg*Tic22 clearly localizes to the periphery of the organelle (Fig. 1*B*). Indeed, the pattern of *Tg*Tic22 localization mirrors that of another peripheral apicoplast protein *Tg*Tic20 (Fig. 1*C*), which localizes to the apicoplast inner membrane (18). Western blot analysis reveals the presence of two bands corresponding to *Tg*Tic22, an upper band of ~60 kDa, and a lower band of ~49 kDa (Fig. 1*D*), indicating N-terminal proteolytic processing.

In plants, Tic22 is a soluble, intermembrane space protein. We analyzed *Tg*Tic22 for transmembrane domains using the TMHMM server (www.cbs.dtu.dk/services/TMHMM). Aside from the N-terminal signal peptide that is cleaved from the mature protein (Fig. 1*D*), *Tg*Tic22 is predicted to lack transmembrane domains. To experimentally test this prediction, we treated *T. gondii* parasites with sodium carbonate at pH 11, separating soluble and peripheral membrane proteins into the supernatant and integral membrane proteins into the insoluble pellet. *Tg*Tic22 partitioned into both soluble and insoluble fractions, whereas the soluble apicoplast protein *Tg*ACP localizes exclusively to the supernatant and the integral membrane apicoplast protein *Tg*Tic20 localizes exclusively to the pellet (Fig. 1*E*). Such a split partitioning in sodium carbonate was also observed with plant Tic22 (14), a protein considered to be soluble. To further address these equivocal results, we extracted *T. gondii* proteins with Triton X-114, and subjected them to phase partitioning into aqueous and detergent phases. *Tg*ACP and *Tg*Tic22 both partition into the aqueous phase, as expected for a soluble protein, while the integral membrane protein *Tg*Tic20 partitions predominantly into the detergent phase. Together, these data suggest that *Tg*Tic22 is a soluble protein of the apicoplast periphery.

TgTic22 Is Essential for Parasite Survival—Despite its predicted role in protein import, the function of plastid Tic22 and its importance to cell survival, have not been addressed. To do so, we generated a conditional mutant of TgTic22 using a previously described system where addition of anhydrotetracycline (ATc) down-regulates transcription of the gene-of-interest (21). An ATc-regulated copy of HA-tagged *Tg*Tic22 was introduced into *T. gondii* parasites retaining the endogenous *Tg*Tic22 gene (iTic22/eTic22). We then engineered a cosmid where the entire *Tg*Tic22-coding region was replaced with a selectable marker (supplemental Fig. S2*A*). We transfected this construct into iTic22/eTic22 parasites and screened for clonal parasites where the native Tic22 gene was disrupted (iTic22/ΔTic22). We verified successful targeting of the locus by PCR and Southern blotting (supplemental Fig. S2*B*).

To test whether we could down-regulate *Tg*Tic22 expression in the mutant, we grew parasites for 0 to 4 days in the presence of ATc and measured the levels of *Tg*Tic22-HA protein by Western blot. We found that *Tg*Tic22-HA was undetectable after 2 days on ATc (Fig. 2*A*). We next introduced tandem tomato red fluorescent protein (RFP) into both the parental (iTic22/eTic22) and mutant (iTic22/ΔTic22) cell lines, and measured parasite growth rates using a sensitive fluorescence growth assay (18). In the absence of ATc, both parental and

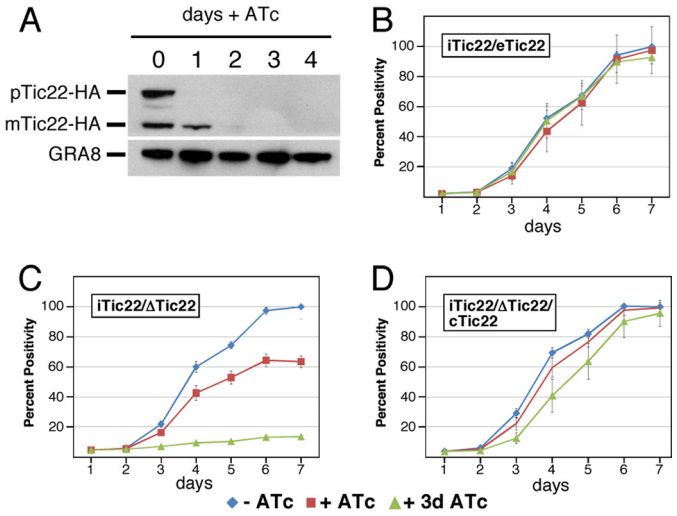

FIGURE 2. **TgTic22 is essential for parasite growth.** *A*, Western blot of inducible *Tg*Tic22-HA expressing parasites grown for 0 to 4 days in ATc. GRA8 serves as a loading control. *B–D*, fluorescence growth assays to monitor the daily growth of parental (*B*), mutant (*C*), and complemented parasites (*D*) in the absence (*blue*) or presence (*red*) of ATc, or preincubated in ATc for 3 days before commencing the assay (*green*). Values represent percent positivity, where the fluorescence of parasites grown in the absence of ATc on the final day (day 7) of the assay is set to 100. Error bars represent one standard deviation from the mean of triplicate samples.

mutant cell lines grow normally (Fig. 2, *B* and *C*). Growth of the parental strain is unaffected after the addition of ATc, but growth of the mutant begins to slow after about 4 days incubation in ATc and ceases after about 6 days. When we pre-incubated parasites for 3 days in ATc before commencing the assay, we see normal growth in the parental cell line, but negligible growth in the mutant. To confirm that the observed growth phenotype is directly due to knockdown of *Tg*Tic22, we introduced a copy of *Tg*Tic22 expressed from a constitutive promoter into the mutant cell line (iTic22/ΔTic22/cTic22). Complementation restores parasite growth in the presence of ATc (Fig. 2*D*). We conclude that *Tg*Tic22 is essential for parasite growth.

TgTic22 Is Required for Apicoplast Protein Import—Given the association of plant Tic22 with plastid-targeted proteins and TIC and TOC complex components (12, 14) we hypothesized that *Tg*Tic22 has a role in apicoplast protein import. When apicoplast proteins are imported into the organelle, the N-terminal targeting peptide is cleaved, probably by a stromal processing peptidase (23). Cleavage serves as a robust marker for successful import. To measure import in Tic22 mutant parasites, we radiolabeled parasites for 1 h with ^{35}S-labeled methionine and cysteine (pulse). We then removed radiolabel and incubated parasites for a further two hours (chase) before immunopurifying the apicoplast protein *Tg*Cpn60 from both pulse and chase samples. Proteins were separated by polyacrylamide gel electrophoresis and purified proteins were detected by autoradiography and phosphorimaging. In parasites grown in the absence of ATc, *Tg*Cpn60 appears as a precursor band after a one-hour pulse, and a large proportion is converted to the smaller, processed form after the chase (Fig. 3*A*). After 2 days on ATc, when *Tg*Tic22 is no longer detectable by Western blot (Fig. 2*A*), there is a considerable reduction in the level of processed *Tg*Cpn60, consistent with an impairment of protein

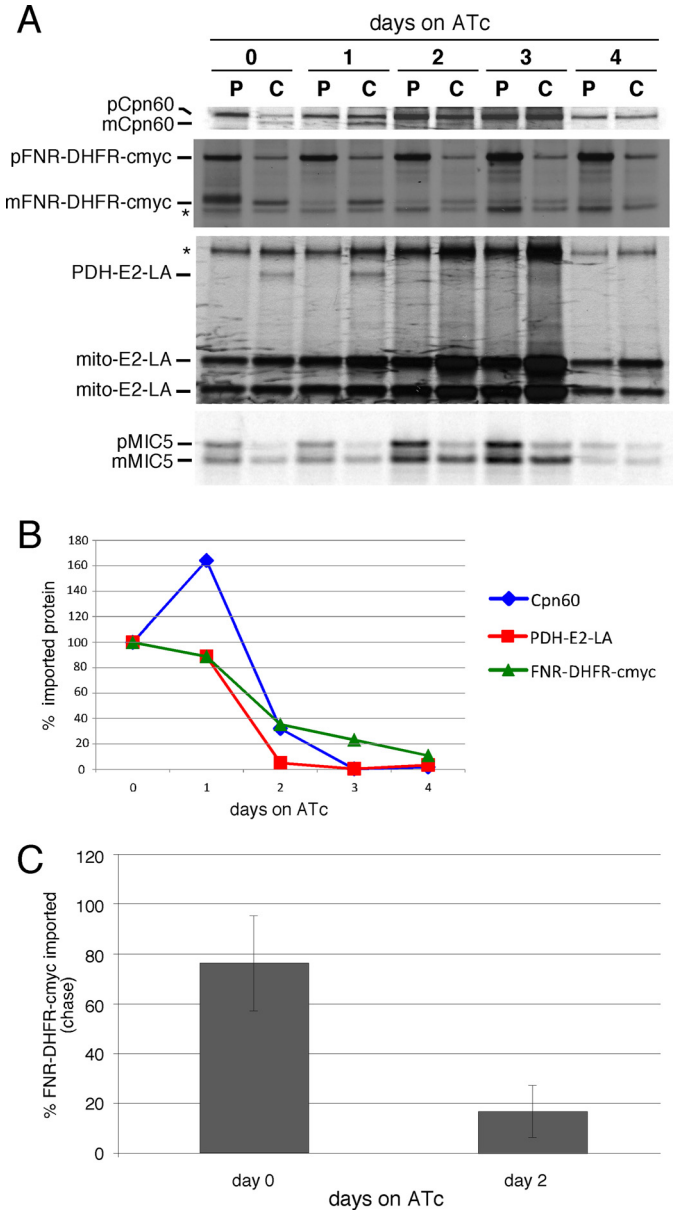

FIGURE 3. **TgTic22 is required for apicoplast protein import.** *A*, pulse-chase analysis of immunopurified proteins extracted from parasites grown for 0 to 4 days on ATc. Proteins were extracted after a 1-h incubation in radioactive methionine and cysteine (*P*), and again after washing out the radiolabel and incubating in non-radioactive medium for 2 h (*C*). We identified precursor and mature forms of the apicoplast stromal proteins *Tg*Cpn60 and FNR-DHFR-cmyc, lipoylated parasite proteins, including the E2 subunit of the apicoplast stromal protein pyruvate dehydrogenase (PDH-E2-LA), and two parasite mitochondrial E2 proteins, and precursor and mature forms of the micronemal protein MIC5. The band marked by an *asterisk* in the c-myc pulldown lanes likely results from the use of an alternative internal start codon representing a shorter cytosolic version of FNR-DHFR-cmyc (18). The asterisk in the lipoic acid pulldowns represents a contaminating host cell protein (18). *B*, quantification of the level of apicoplast targeting of *Tg*Cpn60 (*blue*), PDH-E2-LA (*red*), and FNR-DHFR-cmyc (*green*) seen in the experiments represented in Fig. 3*A*. Samples were quantified relative to the degree of import in the no ATc samples (see "Experimental Procedures"). *C*, quantification of the level of apicoplast targeting of FNR-DHFR-cmyc in parasites grown in the absence of ATc or in the presence of ATc for 2 days. Import levels are expressed as a percentage of imported protein in the chase samples (supplemental Fig. S3) compared with precursor levels in the pulse samples. Error bars indicate one standard deviation from the mean based on three independent replicates.

import into the apicoplast (Fig. 3*A*, *top*, *lane 6*). We quantified levels of *Tg*Cpn60 import by comparing the ratio of the mature protein in the chase lane to precursor in the pulse lane, with the day 0 value set to 100%. This revealed that after 2 days, import is reduced to 32% of control levels and to negligible levels by day 3 (Fig. 3*B*). A loss of some *Tg*Cpn60 in the day 0 chase during sample processing means that the degrees of protein import in subsequent days (*e.g.* the 160% value observed at day 1) are likely an overestimate of the true level of import. As a further measure of apicoplast protein import, we introduced a transgenic apicoplast marker protein (FNR-DHFR-cmyc) previously used to measure apicoplast protein import (18). Much like *Tg*Cpn60, FNR-DHFR-cmyc is processed to the mature form in the absence of ATc (Fig. 3*A*). After 2 days growth on ATc, the amount of mature FNR-DHFR-cmyc is reduced to around 35%, the level in parasites grown in the absence of ATc, and this level decreases to 23% at days 3 and 11% at day 4 (Fig. 3*B*).

As a final measure for apicoplast protein import, we monitored the lipoylation of the E2 subunit of the apicoplast enzyme pyruvate dehydrogenase (PDH-E2), a process that occurs only after protein import into the organelle (18). We purified all parasite lipoylated proteins from both pulse and chase samples using an anti-lipoic acid antibody. In the absence of ATc, lipoylated PDH-E2 appears after the two-hour chase (Fig. 3*A*). After 2 days growth on ATc, the level of lipoylated PDH-E2 is reduced to 5% of the wild-type level, and by day 3 is no longer detectable (Fig. 3, *A* and *B*), again consistent with a defect in apicoplast protein import.

These three measures of apicoplast protein import all indicate a severe effect on import in the absence of *Tg*Tic22. To better quantify the effects of *Tg*Tic22 loss on apicoplast protein import we re-performed the FNR-DHFR-cmyc import assay in triplicate, measuring levels of apicoplast protein import in the absence of ATc or in parasites grown for 2 days in ATc (supplemental Fig. S3). In the absence of ATc, 76% of the precursor protein in the pulse is imported into the apicoplast during the chase, while this value drops to 17% in the absence of Tic22 (Fig. 3*C*). These data indicate that the effect of *Tg*Tic22 on apicoplast protein import is consistent and reproducible.

Mitochondrial protein import is unaffected by *Tg*Tic22 loss, as evidenced by successful lipoylation of mitochondrial E2 subunits in the absence of *Tg*Tic22 (Fig. 3*A*). Trafficking to the apicoplast is initiated at the endoplasmic reticulum and proceeds through the endomembrane system. To rule out a general defect in endomembrane trafficking, we monitored N-terminal cleavage of MIC5. MIC5 traffics to the micronemes, an endosomal compartment, and is N-terminally processed in a pre-micronemal endosomal vacuole (24). ATc had no effect on processing of MIC5 (Fig. 3*A*). Together, the mitochondrial and micronemal data suggest that the effect *Tg*Tic22 knockdown is specific to apicoplast protein import.

We next examined the role of *Tg*Tic22 in apicoplast biogenesis. We found that *Tg*Tic22 knockdown leads to defects in apicoplast biogenesis 1 day after the observed defect in apicoplast protein import (supplemental Fig. S4).

The Structure of Tic22—To gain structural insight into the function of Tic22 we screened homologues from *T. gondii*, *P. falciparum*, and plants (*Pisum* and *Arabidopsis*) for expression, purification and crystallization. Plant Tic22 proteins expressed in *E. coli* were insoluble. *Tg*Tic22 could be successfully expressed and purified, but failed to crystallize, perhaps as a result of the N-terminal extension and low complexity insertions (supplemental Fig. S1). However, we succeeded in expressing residues 68–279 of *Pf*Tic22, corresponding to the predicted mature form (17), and were able to generate crystals. Microseeding allowed the growth of large, single crystals of seleno-methionine labeled protein that diffracted to 2.15 Å resolution (20). A three wavelength MAD dataset was collected, allowing phase determination and building of a final model containing the majority of the protein (residues 68–151 and 162–275).

*Pf*Tic22 is a monomer containing seven α-helices and two four stranded β-sheets (Fig. 4*A*). Four of the major helices are arranged as a cross, forming a mostly planar surface. On top of this lie two β-sheets, each consisting of one pair of parallel and one pair of antiparallel β-strands. Finally three small α-helices top the architecture. Although the structure initially appears pseudodimeric, strands cross between the two halves of the molecule, making it unlikely that this apparent symmetry has arisen from gene duplication. The fold closely resembles that of a cyanobacterial Tic22 homologue (15) but is otherwise unique, suggesting its origins as a periplasmic protein from a cyanobacterial ancestor.

The most striking features of the surface of *Pf*Tic22 are two 30–40Å long grooves, located on either side of the molecule. Intriguingly, when we plotted conserved residues of Tic22 from algal, plant and parasite species (supplemental Fig. S1) onto the surface of the structure, most were located within these two grooves, and similar grooves are found on the bacterial Tic22 homologue (15) (Fig. 4*B*). The grooves also contain the major accumulation of non-polar residues on the protein surface with conserved residues being predominately hydrophobic in nature (supplemental Fig. S5).

Tic22 Mediates in Vitro Chaperone Function through Hydrophobic Grooves—Conserved hydrophobic grooves are found in a number of small chaperones whose role is to maintain proteins in an unfolded state during transport (25, 26). To determine whether *Pf*Tic22 can act as a chaperone, we used an insulin-aggregation assay. The addition of reducing agent to insulin leads to dissociation of the A and B chains and to subsequent aggregation of the B chain, an effect that can be measured by increased light scattering at 360 nm. Chaperone proteins such as SecB, Atp11p or HSP90 can interact with exposed hydrophobic surfaces and prevent B chain aggregation (27–29).

The ability of *Pf*Tic22 to prevent insulin aggregation was tested by following the increase in light scattering at 360 nm. *Pf*Tic22 was mixed with insulin in different ratios, with insulin aggregation initiated by addition of the reducing agent DTT. *Pf*Tic22 reduced insulin aggregation in a concentration-dependent manner. Four *Pf*Tic22 molecules per insulin chain were sufficient to completely block development of light scattering and two molecules per insulin chain led to a 60% decrease (Fig. 5*A*). To assess whether this is a conserved property of Tic22 we also tested *Tg*Tic22. Here the effect was even stronger, with a *Tg*Tic22:insulin ratio of 0.5:1 able to prevent insulin aggregation (Fig. 5*B*). These ratios are comparable to other chaperone

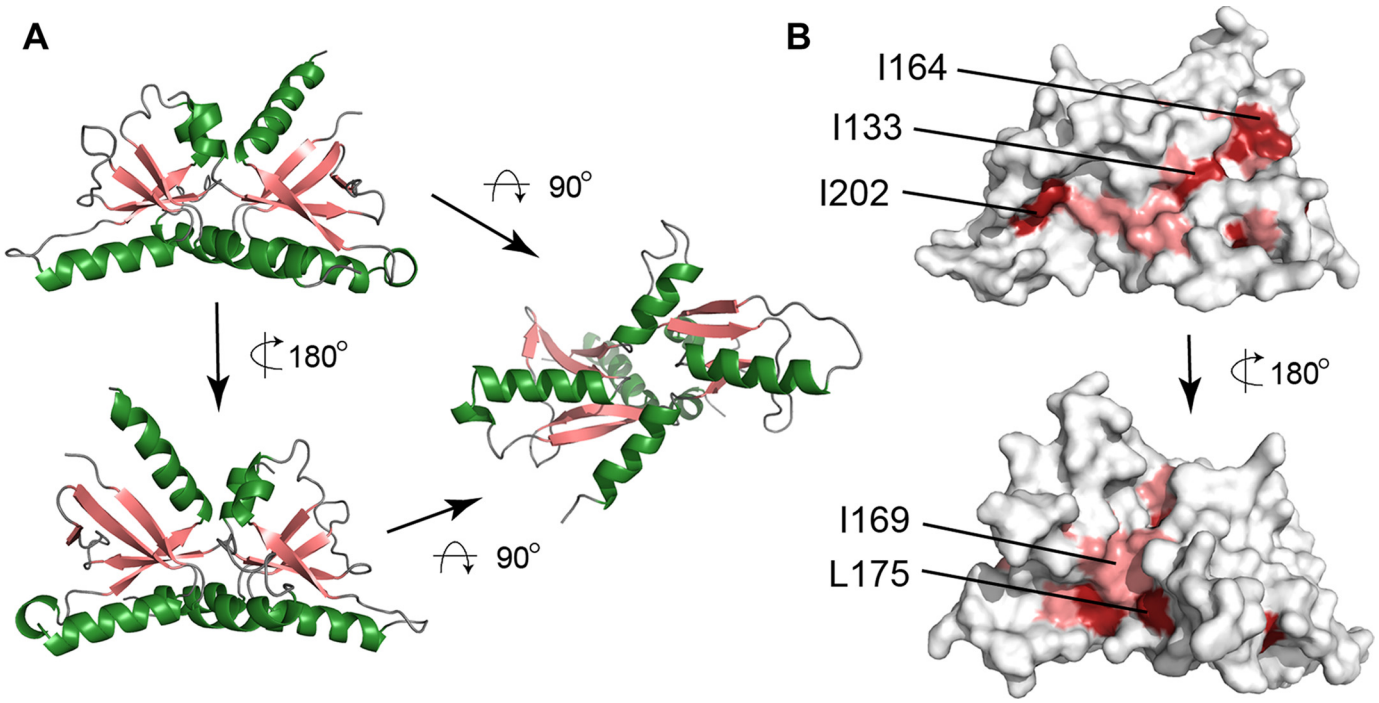

FIGURE 4. *A*, structure of *Pf*Tic22. *B*, conserved residues line two grooves on the surface of *Pf*Tic22 with darker shades of *red* indicating a greater degree of conservation and lighter shades indicating weaker conservation, as illustrated in supplemental Fig. S1.

proteins characterized using this assay, with 1:1 chaperone:protein ratios required to prevent aggregation for SecB and HSP90 and a 2:1 ratio for αA-crystallin (27–30). We conclude that Tic22 has chaperone activity.

We next evaluated the role of the hydrophobic grooves in mediating the chaperone activity of *Pf*Tic22. Five hydrophobic residues were selected (with Ile-169 and Leu-175 from the vertical groove and Ile-133, Ile-164, and Ile-202 from the horizontal groove (Fig. 4*B*)) and were mutated to a hydrophilic serine. The mutant proteins were indistinguishable from wild type protein during purification and by circular dichroism (supplemental Fig. S6), suggesting no changes in structure or aggregation properties. The mutant proteins were tested for their ability to prevent insulin aggregation at a Tic22:insulin ratio of 4:1. While mutation of residues in both hydrophobic grooves reduced chaperone activity (Fig. 5*C*), the largest effects were from mutation of Ile-169 and Leu-175 in the vertical groove. A double mutant (I169S/L175S) reduced the chaperone activity further. Therefore, at a high chaperone:insulin ratio where complete inhibition of aggregation is observed for wild type protein, point mutations in the hydrophobic grooves can significantly reduce chaperone activity. We conclude that Tic22 shows a conserved chaperone activity, mediated by hydrophobic grooves.

DISCUSSION

In this study we use genetic and structural approaches to define the function of Tic22, a molecule with a predicted role in protein import in both plant chloroplasts and apicomplexan apicoplasts. We demonstrate that, as with its plant homologues, *Tg*Tic22 is likely a soluble protein that localizes to the organellar periphery. Four membranes surround the apicoplast, and analogy with chloroplasts predicts that Tic22 may localize to the space between the inner two membranes. *Tg*Tic22 exists as both pre-processed and N-terminally processed isoforms, as is also the case for Tic22 homologues in plants and *P. falciparum*, with the N-terminal extension likely functioning as a plastid-targeting domain (12, 17).

Tic22 has been postulated to play a role in protein import into plastids based on its association with precursor proteins and components of the TIC and TOC complexes (12, 14). Here, we utilize the robust genetics of *T. gondii* to demonstrate for the first time for any organism that cells deficient in Tic22 are impaired in plastid protein import. Loss of *Tg*Tic22 corresponds with a considerable reduction in apicoplast protein import, at a time when cell growth, apicoplast biogenesis and endosomal protein targeting are all unaffected. This supports a direct role for *Tg*Tic22 in apicoplast protein import. In contrast to cyanobacterial Tic22, which is proposed to play a specific role in bacterial outer membrane protein insertion (15), Tic22 has a more ubiquitous role in the apicoplast, with its disruption affecting import of all tested proteins into the stroma. Examining the role of *Tg*Tic22 in biogenesis of *Tg*Toc75 will now be of particular interest to see if this function is conserved from its cyanobacterial counterpart.

As with other apicoplast import mutants we have generated in *T. gondii* (*e.g.* *Tg*Tic20 and *Tg*Der1), loss of apicoplast import is promptly followed by major defects in apicoplast biogenesis (18, 20), consistent with the importance of apicoplast-localized proteins for organellar maintenance. The loss of apicoplasts is the most likely reason for the subsequent inhibition of parasite growth in *Tg*Tic22-less parasites.

The structure of *Pf*Tic22 reveals a fold with hydrophobic grooves on both sides of the molecule. The same has recently been observed for a periplasmic Tic22 homologue from a cya-

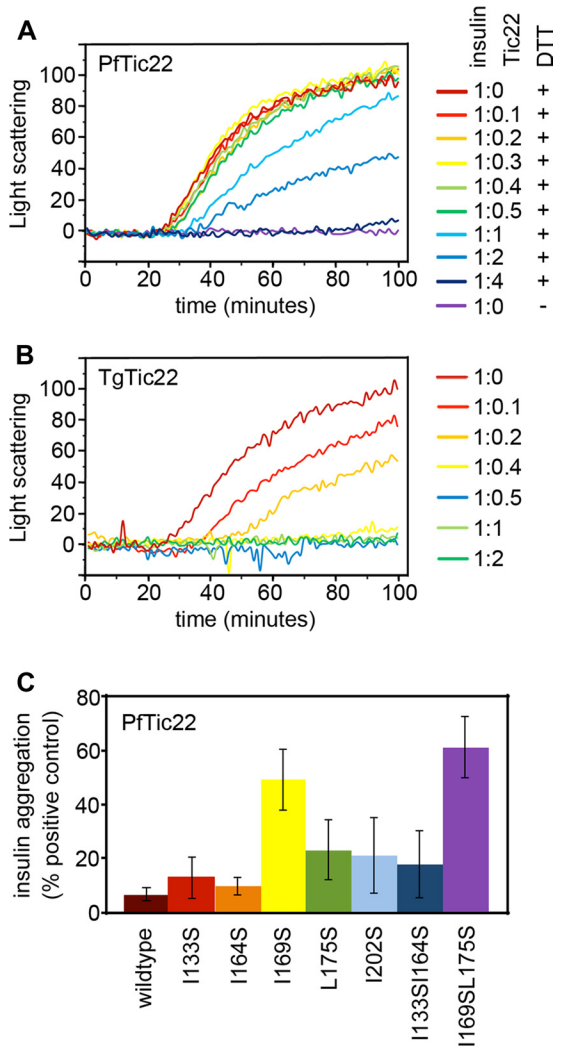

FIGURE 5. **Tic22 acts as a chaperone.** Light scattering due to aggregation of insulin was observed after DTT addition in the presence of different insulin: Tic22 ratios for *A*, *Pf*Tic22 and *B*, *Tg*Tic22. Increasing quantities of Tic22 prevented the development of light scattering by preventing aggregation. *C*, effect of point mutations on the chaperone activity of *Pf*Tic22 reveals that mutations in both hydrophobic grooves reduce the capacity of Tic22 to prevent insulin aggregation, with a double mutant in the vertical groove (I169S/L175S) having the greatest effect.

nobacteria suggesting it to be an ancient fold conserved from cyanoabacteria to plants (15), but has been observed in no other protein. We demonstrate here that the hydrophobic grooves are critical to allow Tic22 to function as a nonspecific, ATP-independent chaperone, preventing aggregation of a model protein. Although we have only tested apicoplast Tic22s for chaperone function, these grooves are also present in plant Tic22 and most likely have the same properties.

Holdases are ATP-independent chaperones that prevent aggregation of their binding partners and are important components of many protein import or secretion systems. Bacteria use a cytosolic chaperone, SecB, that stabilizes unfolded proteins in a suitable state for insertion into the SecYEG translocon. Gram-negative bacteria also contain chaperones in the periplasm, with both SurA and Skp interacting with outer membrane proteins to keep them unfolded and primed for membrane insertion (31). Similarly the mitochondrial intermembrane space contains Tim9-Tim10 and Tim8-Tim13 chaperone complexes. These tiny TIM complexes associate with a subset of imported proteins as they emerge from the outer membrane TOM complex, and deliver them to an inner membrane translocon (32).

While a number of ATP-dependent chaperones play a role in trafficking through the TOC and TIC complex, including a putative intermembrane space Hsp70, no holdase has yet been discovered in this system. Our data demonstrate that Tic22 prevents protein aggregation in an ATP-independent, concentration-dependent manner. We therefore propose that Tic22 acts as such a chaperone in the intermembrane spaces of plant, algal, and apicomplexan plastids, maintaining proteins in an unfolded state during translocation between the inner and outer membranes.

Structural studies of holdases show that diverse features are used for function, but in each case surface exposed non-polar patches on the chaperone are available to interact with aromatic or non-polar residues from target proteins to reduce the driving force for folding and aggregation. In the case of SecB, two long hydrophobic grooves perform this function (26), while Skp and the complex of Tim9 and Tim10 adopt jelly-fish like structures with the inside surfaces of the tentacles providing a hydrophobic environment in which unfolded proteins can be held (33, 34). Dynamic re-association can also be involved, with SurA adopting a variety of quaternary structures, forming different hydrophobic channels to allow interaction with different unfolded protein components (25). In the case of Tic22, exposed hydrophobic grooves are likely to bind to exposed hydrophobic residues on unfolded target proteins, maintaining them in solution. Although Tic22 is a monomer in the crystals, it shows a propensity to form dimers and higher order oligomers when studied in solution by analytical ultracentrifugation, with the dimer as the predominant species for *Pf*Tic22 (supplemental Fig. S7). Whether or not this oligomerization contributes to chaperone function, as seen in SurA (25), is uncertain.

Whether Tic22 is required only for the import of a subset of proteins or more universally is also uncertain. SecB is used ubiquitously in delivery of unfolded proteins to the SecYEG translocon (31), but the use of chaperones in the mitochondrial intermembrane space is limited to a subset of inner membrane proteins (32). Cyanobacterial Tic22 appears to play a role in outer membrane biogenesis (15), and plastid Tic22 may have a similar function. However, *Tg*Tic22 ablation disrupts import of all stromal-targeted proteins tested to date, arguing for a more universal role in plastids. This suggests that a bacterial chaperone with a role in outer membrane biogenesis had been adopted in plastids as a chaperone used to maintain proteins in a translocation-competent state during transit across the inner membrane space. Regardless of whether it is ubiquitously used or required for more specific import pathways, the chaperone Tic22 is clearly critical for both plastid protein import and cell survival.

Acknowledgments—We thank Gary Ward (University of Vermont) and Vern Carruthers (University of Michigan) for sharing antibodies, and Jack de Puit (Campbell High School, ACT, Australia) for assistance with microscopy.

REFERENCES

1. McFadden, G.I., and van Dooren, G. G. (2004) Evolution: red algal genome affirms a common origin of all plastids. *Curr. Biol.* **14,** R514–R516
2. Ralph, S. A., van Dooren, G. G., Waller, R. F., Crawford, M. J., Fraunholz, M. J., Foth, B. J., Tonkin, C. J., Roos, D. S., and McFadden, G. I. (2004) Tropical infectious diseases: Metabolic maps and functions of the *Plasmodium falciparum* apicoplast. *Nat. Rev. Microbiol.* **2,** 203–216
3. Soll, J., and Schleiff, E. (2004) Protein import into chloroplasts. *Nat. Rev. Mol. Cell Biol.* **5,** 198–208
4. Schleiff, E., Jelic, M., and Soll, J. (2003) A GTP-driven motor moves proteins across the outer envelope of chloroplasts. *Proc. Natl. Acad. Sci. U.S.A.* **100,** 4604–4609
5. Scott, S. V., and Theg, S. M. (1996) A new chloroplast protein import intermediate reveals distinct translocation machineries in the two envelope membranes: energetics and mechanistic implications. *J. Cell Biol.* **132,** 63–75
6. Vojta, L., Soll, J., and Bölter, B. (2007) Protein transport in chloroplasts, targeting to the intermembrane space. *FEBS J* **274,** 5043–5054
7. Schnell, D. J., and Blobel, G. (1993) Identification of intermediates in the pathway of protein import into chloroplasts and their localization to envelope contact sites. *J. Cell Biol.* **120,** 103–115
8. Kikuchi, S., Oishi, M., Hirabayashi, Y., Lee, D. W., Hwang, I., and Nakai, M. (2009) A 1-megadalton translocation complex containing Tic20 and Tic21 mediates chloroplast protein import at the inner envelope membrane. *Plant Cell* **21,** 1781–1797
9. Kovács-Bogdán, E., Benz, J. P., Soll, J., and Bölter, B. (2011) Tic20 forms a channel independent of Tic110 in chloroplasts. *BMC Plant Biol.* **11,** 133
10. Chou, M. L., Chu, C. C., Chen, L. J., Akita, M., and Li, H. M. (2006) Stimulation of transit-peptide release and ATP hydrolysis by a cochaperone during protein import into chloroplasts. *J. Cell Biol.* **175,** 893–900
11. Kovacs-Bogdan, E., Soll, J., and Bolter, B. (2010) Protein import into chloroplasts: the Tic complex and its regulation. *Biochim. Biophys. Acta* **1803,** 740–747
12. Kouranov, A., Chen, X., Fuks, B., and Schnell, D. J. (1998) Tic20 and Tic22 are new components of the protein import apparatus at the chloroplast inner envelope membrane. *J. Cell Biol.* **143,** 991–1002
13. Kouranov, A., and Schnell, D. J. (1997) Analysis of the interactions of preproteins with the import machinery over the course of protein import into chloroplasts. *J. Cell Biol.* **139,** 1677–1685
14. Becker, T., Hritz, J., Vogel, M., Caliebe, A., Bukau, B., Soll, J., and Schleiff, E. (2004) Toc12, a novel subunit of the intermembrane space preprotein translocon of chloroplasts. *Mol. Biol. Cell* **15,** 5130–5144
15. Tripp, J., Hahn, A., Koenig, P., Flinner, N., Bublak, D., Brouwer, E. M., Ertel, F., Mirus, O., Sinning, I., Tews, I., and Schleiff, E. (2012) Structure and conservation of the periplasmic targeting factor Tic22 from plants and cyanobacteria. *J. Biol. Chem.* **287,** 24164–24173
16. Bullmann, L., Haarmann, R., Mirus, O., Bredemeier, R., Hempel, F., Maier, U. G., and Schleiff, E. (2010) Filling the gap, evolutionarily conserved Omp85 in plastids of chromalveolates. *J. Biol. Chem.* **285,** 6848–6856
17. Kalanon, M., Tonkin, C. J., and McFadden, G. I. (2009) Characterization of two putative protein translocation components in the apicoplast of *Plasmodium falciparum. Eukaryot Cell* **8,** 1146–1154
18. van Dooren, G. G., Tomova, C., Agrawal, S., Humbel, B. M., and Striepen, B. (2008) Toxoplasma gondii Tic20 is essential for apicoplast protein import. *Proc. Natl. Acad. Sci. U.S.A.* **105,** 13574–13579
19. Agrawal, S., van Dooren, G. G., Beatty, W. L., and Striepen, B. (2009) Genetic evidence that an endosymbiont-derived endoplasmic reticulum-associated protein degradation (ERAD) system functions in import of apicoplast proteins. *J. Biol. Chem.* **284,** 33683–33691
20. Glaser, S., and Higgins, M. K. (2012) Overproduction, purification and crystallization of PfTic22, a component of the import apparatus from the apicoplast of. *Plasmodium falciparum*. *Acta Crystallogr. Sect. F Struct. Biol. Cryst. Commun.* **68,** 351–354
21. Brooks, C. F., Johnsen, H., van Dooren, G. G., Muthalagi, M., Lin, S. S., Bohne, W., Fischer, K., and Striepen, B. (2010) The *Toxoplasma* apicoplast phosphate translocator links cytosolic and apicoplast metabolism and is essential for parasite survival. *Cell Host Microbe* **7,** 62–73
22. van Dooren, G. G., Reiff, S. B., Tomova, C., Meissner, M., Humbel, B. M., and Striepen, B. (2009) A novel dynamin-related protein has been recruited for apicoplast fission in *Toxoplasma gondii. Curr. Biol.* **19,** 267–76
23. van Dooren, G. G., Su, V., D'Ombrain, M. C., and McFadden, G. I. (2002) Processing of an apicoplast leader sequence in *Plasmodium falciparum* and the identification of a putative leader cleavage enzyme. *J. Biol. Chem.* **277,** 23612–23619
24. Brydges, S. D., Sherman, G. D., Nockemann, S., Loyens, A., Däubener, W., Dubremetz, J. F., and Carruthers, V. B. (2000) Molecular characterization of TgMIC5, a proteolytically processed antigen secreted from the micronemes of *Toxoplasma gondii. Mol. Biochem. Parasitol.* **111,** 51–66
25. Xu, X., Wang, S., Hu, Y. X., and McKay, D. B. (2007) The periplasmic bacterial molecular chaperone SurA adapts its structure to bind peptides in different conformations to assert a sequence preference for aromatic residues. *J. Mol. Biol.* **373,** 367–381
26. Xu, Z., Knafels, J.D., and Yoshino, K. (2000) Crystal structure of the bacterial protein export chaperone secB. *Nat. Struct. Biol.* **7,** 1172–1177
27. del Valle, L. J., Escribano, C., Pérez, J. J., and Garriga, P. (2002) Calcium-induced decrease of the thermal stability and chaperone activity of α-crystallin. *Biochim. Biophys. Acta* **1601,** 100–109
28. Scheibel, T., Weikl, T., and Buchner, J. (1998) Two chaperone sites in Hsp90 differing in substrate specificity and ATP dependence. *Proc. Natl. Acad. Sci. U.S.A.* **95,** 1495–1499
29. Sheluho, D., and Ackerman, S. H. (2001) An accessible hydrophobic surface is a key element of the molecular chaperone action of Atp11p. *J. Biol. Chem.* **276,** 39945–39949
30. Panse, V. G., Vogel, P., Trommer, W. E., and Varadarajan, R. (2000) A thermodynamic coupling mechanism for the disaggregation of a model peptide substrate by chaperone secB. *J. Biol. Chem.* **275,** 18698–18703
31. Danese, P. N., and Silhavy, T. J. (1998) Targeting and assembly of periplasmic and outer-membrane proteins in *Escherichia coli*. *Annu. Rev. Genet.* **32,** 59–94
32. Chacinska, A., Koehler, C. M., Milenkovic, D., Lithgow, T., and Pfanner, N. (2009) Importing mitochondrial proteins: machineries and mechanisms. *Cell* **138,** 628–644
33. Walton, T. A., and Sousa, M. C. (2004) Crystal structure of Skp, a prefoldin-like chaperone that protects soluble and membrane proteins from aggregation. *Mol. Cell* **15,** 367–374
34. Webb, C. T., Gorman, M. A., Lazarou, M., Ryan, M. T., and Gulbis, J. M. (2006) Crystal structure of the mitochondrial chaperone TIM9.10 reveals a six-bladed α-propeller. *Mol. Cell* **21,** 123–133